

Received October 21, 2019, accepted November 19, 2019, date of publication November 29, 2019,
date of current version December 13, 2019.

Digital Object Identifier 10.1109/ACCESS.2019.2956766

Dual-Mode Noise-Reconstructed EMD for Weak Feature Extraction and Fault Diagnosis of Rotating Machinery

JING YUAN¹, HUIMING JIANG¹, QIAN ZHAO¹, CHONG XU¹, HAIJIANG LIU²,
AND YONGXIANG TIAN³

¹School of Mechanical Engineering, University of Shanghai for Science and Technology, Shanghai 200093, China

²School of Mechanical and Power Engineering, Tongji University, Shanghai 201804, China

³Shanghai Fire Research Institute of MEM, Shanghai 200032, China

Corresponding author: Jing Yuan (yuanjing_802@163.com)

This work was supported in part by the National Natural Science Foundation of China under Grant 51975377, in part by the Shanghai Sailing Program under Grant 18YF1417800, in part by the Key Laboratory of Vibration and Control of Aero-Propulsion System Ministry of Education, Northeastern University under Grant VCAME201907, in part by the Shanghai Special Funds for Industrial Transformation, Upgrading and Development under Grant GYQJ-2019-1-03, and in part by the National Key Research and Development Program of China under Grant 2016YFC0802900.

ABSTRACT The meaningful data-based fault diagnosis is beforehand revealing the potential faults to reduce the costly breakdowns, one challenging of which is extracting the weak features from the complicated signals. Ensemble noise-reconstructed EMD (ENEMD) is an intelligent method by the nice integration of adaptively decomposing and naturally denoising. However, ENEMD still suffers from such issues as the false possible noise-only IMFs and the universal minimax threshold, reducing the precision of the critical noise estimation for the weak feature extraction. Thus, the dual-mode noise-reconstructed EMD method is proposed for weak feature extraction and fault diagnosis of rotating machinery. First, the possible noise-only IMF selection rule is redesigned according to the noise characteristic and the correlation evaluation, to eliminate the redundant slowly oscillating IMFs mistakenly chosen for noise estimation. Second, the adaptive local minimax threshold is proposed in the noise estimation technique for the low SNR signal, to overcome the drawback of additionally keeping some critical but weak fault features into the estimation noise. Hereinto, the local threshold is respectively performed in each sliding window defined by the demodulated rotating-related feature frequency. Third, the proposed method is addressed with the flowchart. Finally, two engineering case studies are implemented to demonstrate the feasibility and effectiveness of the method. The analytic results show that the method could effectively extract the periodic impulses generating by the early local damage in the gearbox of a hot strip finishing mill. Meanwhile, the method could successfully reveal the weak rubbing-impact faults along with alleviating the mode mixing phenomenon in the refined results for fault diagnosis of a heavy oil catalytic cracking unit. Hence, the method could provide a promising tool for weak feature extraction and fault diagnosis of rotating machinery.

INDEX TERMS Empirical mode decomposition, noise reconstruction, weak fault feature, rotating machinery.

I. INTRODUCTION

Machinery fault diagnosis and failure mechanism has a rich history since the 1960s [1], [2]. The fault feature extraction of rotating machinery is always one of the fundamental and vital issues for successful fault diagnosis. Several

The associate editor coordinating the review of this manuscript and approving it for publication was Ruqiang Yan.

efforts have been made to provide a promising tool for the fault feature extraction, mainly concentrated on the adaptive decomposition and denoising methods, such as empirical mode decomposition (EMD) [3], sparse representation [4], local mean decomposition [5], variational mode decomposition [6] and wavelets [7]. Hereinto, EMD is a well-known adaptive decomposition method that decomposes any nonstationary and nonlinear noisy signal into a series of

intrinsic mode functions (IMFs) [8]. Evolving from EMD for addressing such drawbacks as the mode mixing, ensemble EMD (EEMD) with the derivative methods has become an emerging approach and shows the possibility of superior performance in the feature extraction and fault diagnosis of rotating machinery [9], [10].

Despite the nice performance of these methods, most previous investigations focus on the distinct signatures enhanced from the obvious faults or damages. The meaningful and positive data-based fault diagnosis is beforehand revealing the potential faults initiating in the operation to reduce and eliminate the unscheduled downtime and costly breakdowns, one challenging of which is extracting the weak features from the complicated and multiple signals contaminated by the heavy noise and disturbance. Therefore, the weak feature extraction methods and fault diagnosis practices have attracted remarkable attention from researchers [11], [12]. As an intelligent method of simultaneous decomposition and denoising, ensemble noise-reconstructed EMD (ENEMD) is proposed by Yuan and He et al., the IMFs of which are obtained by the ensemble mean of several EMD trials on the noise-reconstructed versions [13]. Different from the traditional noise suppression methods, ENEMD is reconstructing and utilizing the inherent noise to alleviate the mode mixing problem and enhancing the fault features, especially the weak features. To improve the issues of the artificial parameter setup and the poor performance for a high signal-to-noise ratio (SNR) signal, integrated ensemble noise-reconstructed EMD is proposed with the two noise estimation techniques, i.e. by the minimax thresholding for a low SNR case and the local reconfiguration for a high SNR case [14]. Even with the powerful capability of fault signature enhancement and detection, these ENEMD methods still suffer from some issues concerned on the precision of the critical noise estimation for the weak feature extraction. Two major drawbacks are revealed as follows: (1) In the original possible noise-only IMF selection, the IMFs satisfying with the noise-only IMF energies within a certain confidence interval are all treated to be the possible noise-only IMFs for determining the noise estimation strategy or the further thresholding for a low SNR case. However, several slowly oscillating IMFs with the high index are sometimes mistakenly chosen, resulting in the deviation of noise estimation. The false possible noise-only IMFs may markedly influence the weak feature extraction and fault diagnosis. (2) For a low SNR signal, the universal minimax threshold is adopted to refine the inherent noise. Unfortunately, the same level for the same IMF is not suitable for the weak fault features, due to the excess keep of some critical but local weak fault features into the estimation noise.

To overcome the drawbacks, the dual-mode noise-reconstructed EMD method is enhanced from the recent integrated ensemble noise-reconstructed EMD for the weak feature extraction and fault diagnosis of rotating machinery. The main contributions of the manuscript are focused on: (1) The false possible noise-only IMFs are eliminated by calculating the correlation between the possible noise-only and

noise-free components designed by these selected noise-only IMFs. (2) The adaptive local minimax threshold is performed in the noise estimation of the low SNR case, by the sliding window technique defined by the rotating-related feature frequency demodulated from each corresponding IMF. Furthermore, the enhanced method is verified by the fault diagnosis of a hot strip finishing mill and a heavy oil catalytic cracking unit.

The remainder of the paper is organized as follows. A brief introduction of the basic ENEMD is reviewed in Section 2. Section 3 provides the proposed method. In Section 4, the engineering validations are performed. Conclusions are given in Section 5.

II. REVIEW OF ENEMD

ENEMD could offer a physical interpretation for nonstationary and/or nonlinear processes by the integration of adaptive decomposing and natural denoising. Two core concepts of ENEMD are: (1) Unlike EEMD additionally adding the white noise to address the mode mixing problem, the noise inherent in the measure signal is introduced in ENEMD to fundamentally change the local extreme, which helps to project the decomposing components of different scales into their corresponding true IMFs. (2) A set of reconstructed noise versions originated from the measure signal cancels each other out on the approach of the ensemble means, resulting in the improvement on SNR of the fault signal.

The summary of EMD theory involved in ENEMD is referred to Ref. [8]. A measure signal $x(t)$ is generality constituted by a true noise-free signal $s(t)$ and an inherent noise $n(t)$. The algorithm of basic ENEMD is reviewed as follows [13].

- (1) Calculate $\hat{n}(t)$ from $x(t)$ by the noise estimation techniques, where $\hat{\cdot}$ denotes an estimate.
- (2) Reconstruct $\hat{n}(t)$ by randomly permutation and obtain $\hat{s}(t)$ by $\hat{s}(t) = x(t) - \hat{n}(t)$.
- (3) Generate the observed signal $\hat{x}_j(t)$ at the j th version using $\hat{x}_j(t) = \hat{s}(t) + \hat{n}_j(t)$.
- (4) EMD is performed on $\hat{x}_j(t)$ to acquire a set of IMFs $\{c_{j,k}(t), k = 1, \dots, n\}$ and the residual $r_j(t)$, where k represents the IMF index.
- (5) Repeat steps (3) and (4) within r times until the stopping criterion determined by a predetermined error tolerance ε is arrived.
- (6) The ensemble means of these IMFs are output by $\tilde{c}_k(t) = \frac{\sum_{j=1}^r c_{j,k}(t)}{r}$ and $\tilde{r}(t) = \frac{\sum_{j=1}^r r_j(t)}{r}$.

The idea of the basic ENEMD is simple and interesting, however, the challenging of which is revealed to be the precision of the critical noise estimation. In the original ENEMD, the noise estimation by the hard thresholding is performed. In the integrated ENEMD, the noise estimation by the minimax thresholding is developed for a low SNR case and the noise estimation by the local reconfiguration is introduced for a high SNR case. The specific noise estimation techniques can be found in Refs.[13] and [14]. Hereinto,

the noise estimation by the local reconfiguration which would be adopted in the subsequent method is briefly reviewed by Ref.[14].

- (1) Design the optimum phase space \mathbf{X} using the embedding principle, optimized by the correlation minimization.
- (2) Perform singular value decomposition (SVD) on \mathbf{X} to yield the singular values $\{\lambda_i (i = 1, \dots, q)\}$.
- (3) Compute the increment $\Delta SE_i (i = 1, \dots, q - 1)$ of the normalized singular entropy for $\{\lambda_i\}$.
- (4) Determine the critical singular order p by locating ΔSE_i stability after the first drop.
- (5) Generate the refined $\tilde{\lambda}$ by $\lambda = \{0, \dots, 0, \lambda_p, \dots, \lambda_q\}$.
- (6) Achieve the expected $\hat{n}(t)$ using the inverse of SVD.

III. DUAL-MODE NOISE-RECONSTRUCTED EMD

To overcome the aforementioned drawbacks for improving the precision of the critical noise estimation, the proposed method is enhanced from the integrated ENEMD for the weak feature extraction and fault diagnosis. To distinguish from the integrated ENEMD, the proposed method is renamed by dual-mode noise-reconstructed EMD.

A. POSSIBLE NOISE-ONLY IMF SELECTION RULE

In the method, the possible noise-only IMF selection rule is first redesigned to remove the false noise-only IMFs. It is well known that most of the noise always locates in the medium and high frequency band, namely the IMFs with the low indexes. Thus, these false IMFs stratifying the noise-only energy often characterize as the slow oscillation with the high indexes. Based on the noise characteristic, the selected possible noise-only IMFs with the first few successive indexes become a nature part of possible noise-only IMF collection. Meanwhile, the other IMFs with the discontinuous indexes are decided by evaluating their noise properties. The possible noise-only IMF selection rule is described as follow.

- (1) Decompose $x(t)$ using EMD into $\{c_k(t), k = 1, \dots, n\}$ and $r(t)$.
- (2) Calculate the energy $\{E_k, k = 1, \dots, n\}$ of each IMF.
- (3) Suppose $c_1(t)$ to be the noise component, the noise energy $\hat{E}n_1$ is E_1 .
- (4) Estimate the noise energies $\{\hat{E}n_{k,95\%}, k = 2, \dots, n\}$ and $\{\hat{E}n_{k,99\%}, k = 2, \dots, n\}$ for $\{c_k(t), k = 2, \dots, n\}$ with the confidence intervals of 95% and 99% by

$$\hat{E}n_k = \frac{\hat{E}n_1}{\beta} \rho^{-k} \quad (1)$$

where $\beta = 0.719$, $\rho = 2.449$ for $\{\hat{E}n_{k,95\%}\}$ and $\rho = 1.919$ for $\{\hat{E}n_{k,99\%}\}$ [15].

- (5) Compare $\log_2 \{E_k\}$ with $\log_2 \{\hat{E}n_{k,95\%}\}$ and $\log_2 \{\hat{E}n_{k,99\%}\}$. If $\log_2 \hat{E}n_{k,95\%} \leq \log_2 E_k \leq \log_2 \hat{E}n_{k,99\%}$, or $\log_2 \hat{E}n_{k,95\%} - \log_2 E_k \leq \alpha$, or $\log_2 E_k - \log_2 \hat{E}n_{k,99\%} \leq \alpha$ ($\alpha = 1$ in the paper), select the

corresponding $c_k(t)$ into the pending noise-only IMF collection N_{noise} ; otherwise, $c_k(t)$ is chosen to be the possible noise-free IMF.

- (6) In N_{noise} , the first few IMFs $\{c_k(t), k = 1, \dots, m\}$ with the successive indexes from 1 to m are directly treated to be the possible noise-only IMFs, due to the noise characteristic.
- (7) Combine $\{c_k(t), k = 1, \dots, m\}$ to yield the pending noise $np(t)$ along with the pending noise-free signal $sp(t)$ by $sp(t) = x(t) - np(t)$.
- (8) Compute the correlation coefficient cc between $np(t)$ and $sp(t)$.
- (9) For each $c_k(t)$ with the discontinuous index, update $np(t)$ by adding $c_k(t)$ to acquire the reborn $np'(t)$ and $sp'(t)$.
- (10) Refresh cc' by $np'(t)$ and $sp'(t)$. If $cc' \leq cc$, $c_k(t)$ is supposed to be the possible noise-only IMF, and subsequently update $np(t)$, $sp(t)$ and cc ; otherwise, $c_k(t)$ is treated as the possible noise-free IMF.
- (11) Repeat Steps (9) and (10) for all the IMFs with the discontinuous indexes in N_{noise} .
- (12) Construct the collection of all the possible noise-only IMFs obtaining from the above steps, denoted as $\{c_l(t), l = 1, \dots, m, \dots\}$.

B. NOISE ESTIMATION TECHNIQUE BY THE ADAPTIVE LOCAL MINIMAX THRESHOLD

Next, we focus on the noise estimation technique for the low SNR signal, one drawback of which is the universal minimax threshold disability for the weak feature extraction. Due to the rotating characteristic, the weak features are represented as the rotating-related feature frequencies, which are always modulated to the system nature frequencies. Hence, the rotating-related feature frequencies demodulated from IMFs are introduced to design the sliding window and then segment each corresponding IMF into a series of periodic sub-signals. The local noise estimation is performed in each window using the local minimax threshold comprehensively determined by the energy and length of each window. The noise estimation technique by the adaptive local minimax threshold for a low SNR signal is described as follows.

- (1) According to the aforementioned possible noise-only IMF selection rule, $\{c_l(t), l = 1, \dots, m, \dots\}$ are chosen to be dealt with.
- (2) For each $c_l(t)$, the rotating-related frequency f_l is demodulated from $c_l(t)$ by locating the maximum value of the envelope demodulation spectrum.
- (3) The adaptive sliding window for $c_l(t)$ is restricted by the width $w_l = f_s/f_l$, where f_s denotes the sampling frequency and w_l is rounded.
- (4) The sub-signals in the sliding windows of $c_l(t)$ is given by

$$window_l(i) = \{c_l(t), t = 1 + iw_l, \dots, (i + 1)w_l\}, \quad i = 0, \dots, nn/w_l - 1 \quad (2)$$

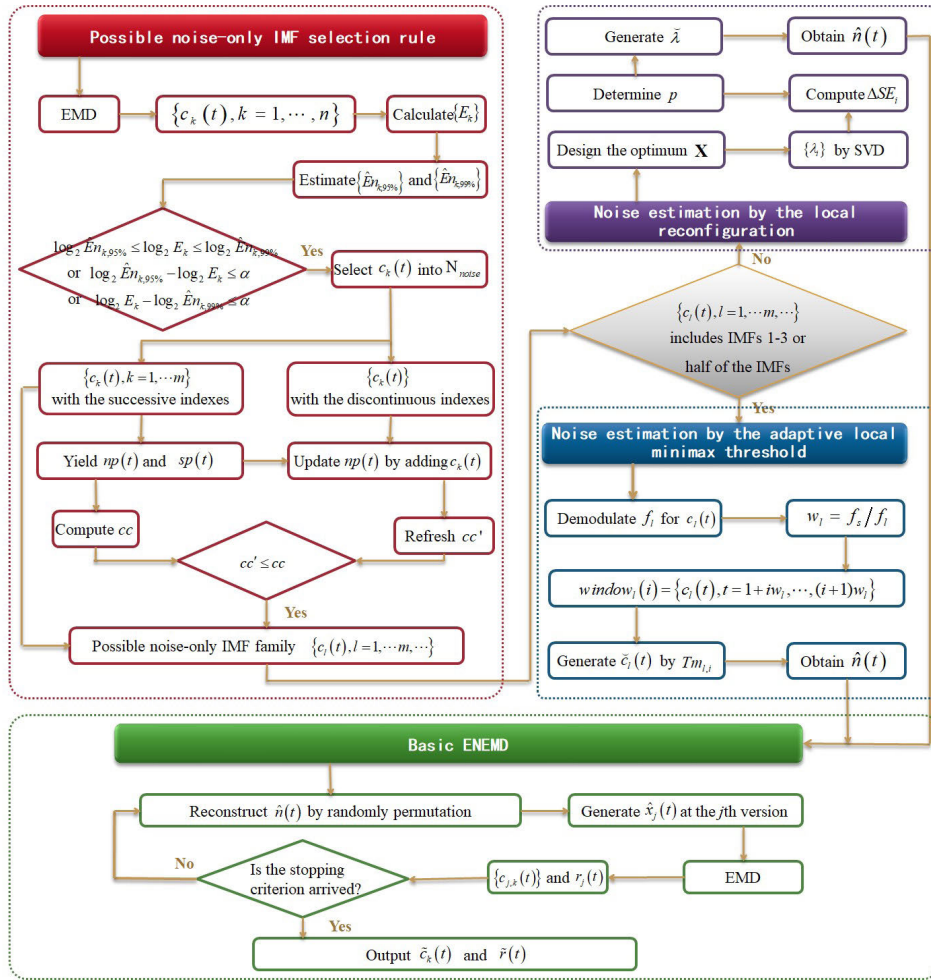


FIGURE 1. The flowchart of the proposed method.

where, the length of $c_l(t)$ is nm . Note that, if the remainder coefficients of $c_l(t)$ at the right boundary are not enough for w_l , the last window is replenished by zeros.

- (5) Generate the refined noise sample $\check{c}_l(t)$ by the local minimax thresholding in each $window_l(i)$ by

$$\check{c}_l(t) = \begin{cases} c_l(t) & |c_l(t)| \leq Tm_{l,i} \\ 0 & |c_l(t)| > Tm_{l,i} \end{cases} \quad (3)$$

The local minimax threshold $Tm_{l,i}$ for $window_l(i)$ is defined below inspired by the minimax estimation of wavelet shrinkage [16], where $E_{l,i}$ is the energy of each $window_l(i)$ calculating by the component median [17].

$$Tm_{l,i} = \begin{cases} \sqrt{E_{l,i}} (0.3936 + 0.1829 \log_2 w_l) & w_l > 32 \\ 0 & w_l \leq 32 \end{cases} \quad (4)$$

- (6) Recombine the refined noise for each $c_l(t)$ by the inverse transformation of Step (4).
- (7) Generate the expected $\hat{n}(t)$ using $\hat{n}(t) = \sum_l \check{c}_l(t)$.

C. THE PROPOSED METHOD

Up to now, the possible noise-only IMF selection rule and the noise estimation technique by the adaptive local minimax threshold for a low SNR signal have been addressed for the weak feature extraction and fault diagnosis. Because the weak feature in a high SNR signal is relatively evident and easy to detect, the noise estimation technique by the local reconfiguration is directly employed in the proposed method. To sum up, the algorithm of the dual-mode noise-reconstructed EMD is condensed as the following steps, whose flowchart is illustrated by Fig.1.

- (1) Implement the possible noise-only IMF selection rule to yield $\{c_l(t), l = 1, \dots, m, \dots\}$, according to the steps in Sec.III(A).
- (2) If $\{c_l(t), l = 1, \dots, m, \dots\}$ includes IMFs 1-3 or half of the IMFs, the noise estimation by the adaptive local minimax threshold for a low SNR signal is conducted following the steps in Sec.III(B).
- (3) For the rest case, the noise estimation by the local reconfiguration is carried out following the steps in Sec.II.

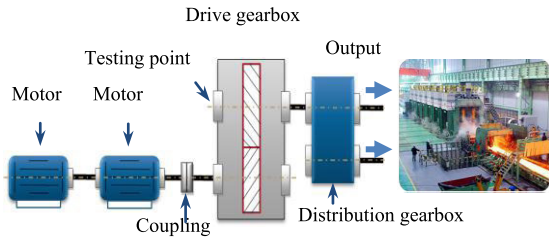


FIGURE 2. The structural sketch of the main drive system of the fifth mill.

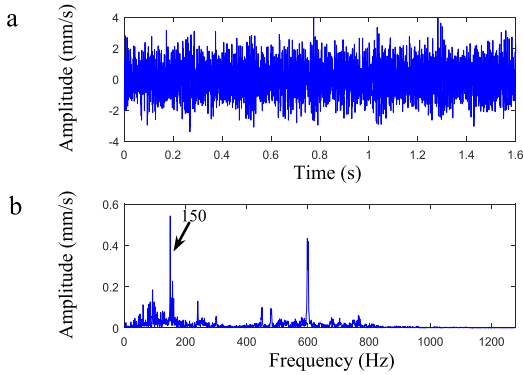


FIGURE 3. (a) A collected signal in case 1; (b) The Fourier spectrum.

- (4) Perform the steps of basic ENEMD in Sec.II to finally output the analytic results by $\{\tilde{c}_k(t)\}$ and $\tilde{r}(t)$.

IV. ENGINEERING VALIDATIONS

The proposed method is applied to the weak fault diagnosis of gearbox for a hot strip finishing mill and the early rub-impact fault diagnosis of a heavy oil catalytic cracking unit. For comparison, the original ENEMD, EEMD and EMD are employed to analyze the same faulty data. In ENEMD, the parameters are chosen to be $\varepsilon = 0.01$ the same as the proposed method and $C = 0.4$. In EEMD, we set the amplitude of the adding noise to be 0.1 times of the standard deviation of the original data and the ensemble number to be 50.

A. CASE 1: GEARBOX FAULT DIAGNOSIS OF A HOT STRIP FINISHING MILL

Fault diagnosis of finishing mills plays a critical role in improving the high quality of steel products and the operation safety guarantee. Gearboxes are the kernel drive systems for finishing mills. Due to the complicated and severe operating condition with heavy loads, the gearbox faults generating in the mills are always contaminated by a large amount of background noise and multiple interference sources from the whole rolling line. Thus, the proposed method is introduced to extract the weak features for the fault diagnosis of finishing mills. A hot strip finishing mill line contains seven frames of rolling mills. The main drive system in the fifth mill contains a single-stage gearbox with Z30/Z39, whose structural sketch is shown in Fig.2. In a routine point inspection, the velocity signals were measured on the outer case of the gearbox close to the large gear during the finishing rolling by a handheld

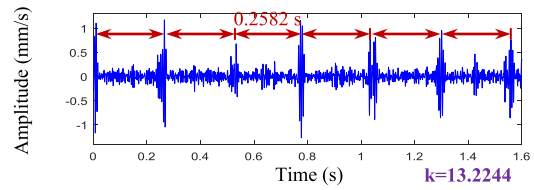


FIGURE 4. The refined result in case 1 by the proposed method.

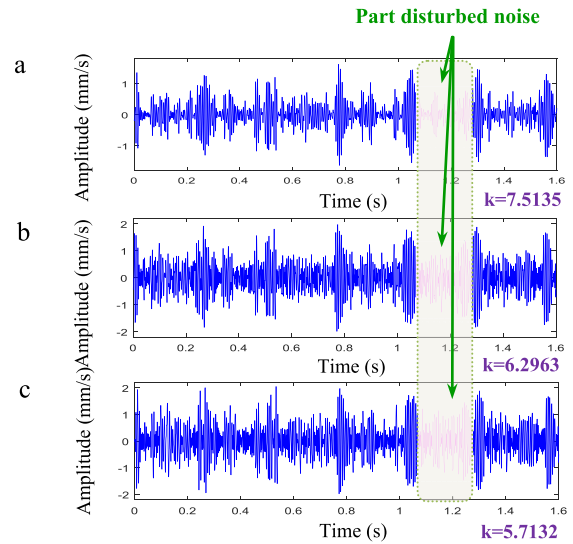


FIGURE 5. The refined results in case 1 by: (a) the original ENEMD; (b) EEMD; (c) EMD.

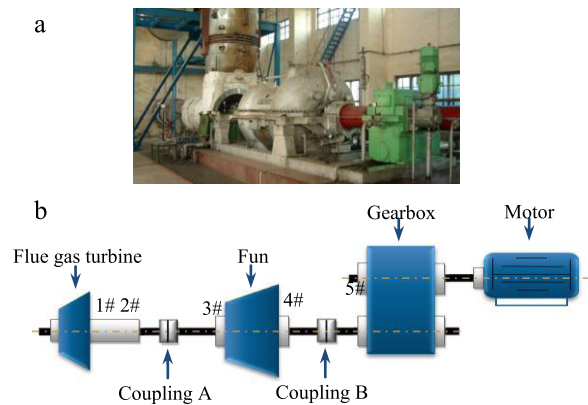


FIGURE 6. The heavy oil catalytic cracking unit: (a) the photograph; (b) the structural sketch.

data acquisition instrument. Due to the variable working condition of the whole finishing rolling, the signals were collected in the middle of the nonstationary process sampled at 2560 Hz. Meanwhile, the actual rotating frequencies of the gearbox are conveniently computed from the meshing frequency in engineering practice. A collected signal and its Fourier spectrum are plotted in Fig.3. The meshing frequency 150 Hz is easy to identify from the spectrum. Thus, the rotating frequencies of the pinion and large gear are respectively calculated at 5 Hz and 3.846 Hz. Several impulsive series are present in the signal, nevertheless the monitoring indexes of which are within the normal limits.

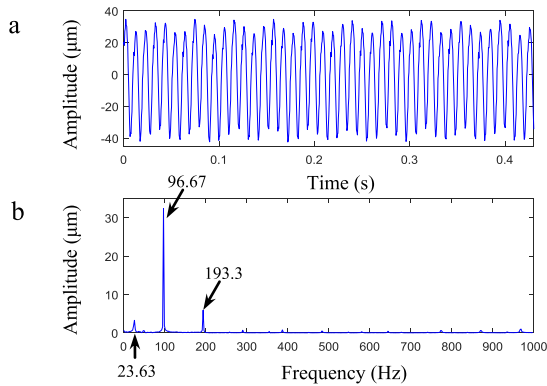


FIGURE 7. (a) A taken signal in case 2; (b) The Fourier spectrum.

We apply the proposed method to analyze the signal in Fig.2(a), following the flowchart of Fig.1. According to the possible noise-only IMF selection rule, $\{c_l(t), l = 1, 2, 3, 4, 10\}$ are selected to estimate the noise, removing the false components $\{c_l(t), l = 8, 9\}$ from the original ENEMD. Containing IMFs 1-3, the noise estimation by the adaptive local minimax threshold for a low SNR signal is conducted. Hereinto, $\{f_l = 19.38, 3.75, 7.5, 18.75, 0.625 \text{ Hz}\}$ which are most relative to the rotating frequencies of the pinion and large gear, are demodulated from $\{c_l(t)\}$ and then determines $\{w_l\}$. In the analysis results, a series of periodic impulses are apparent in IMF3, which we display in Fig.4. The average period is approximately equal to 0.2582 s, whose inverse is close to the rotating frequency of the large gear. The distinct extracted features indicate the localized fault in the large gear, such as a crack, spalling or wear.

We also use the contrastive methods to analyze the same signal, whose feature results are plotted in Fig.5. Although the fault signatures could be captured, they are still disturbed by the noise (part noise highlighted in the rectangle). Obviously, the periodic features extracted by the proposed method are much more distinct without disturbing than those by the contrastive methods. Furthermore, the kurtosis values of the feature results in Figs.4-5 are calculated and shown as the k symbol in these figures. The kurtosis value by the proposed method is much higher than those by the contrastive methods. Thus, the analytic result by the proposed method could provide the undoubted fault symptoms for the fault diagnosis and easily recognized by the factory operators.

Because of the monitoring indexes within the normal limits, the localized fault was conjectured to be the potential fault possible in the early fault stage. The gearbox was monitoring and still operating for a few weeks. In the monthly overhauling, a wear fault was found on the large gear of the gearbox, consistent with the diagnostic conclusion by the proposed method.

B. CASE 2: RUB-IMPACT FAULT DIAGNOSIS OF A HEAVY OIL CATALYTIC CARCKING UNIT

A heavy oil catalytic cracking unit is one of the significance equipment in an oil refinery. One heavy oil catalytic cracking

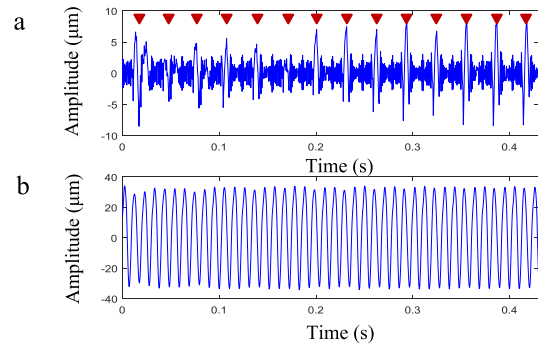


FIGURE 8. The refined results in case 2 by the proposed method: (a) IMF1; (b) IMF2.

unit is constituted by a motor, a gearbox, a fan, a flue gas turbine, couplings and bearing bushes, whose photograph and structural sketch are illustrated in Fig.6. Five eddy current sensors were mounted on the outer case of the bearings to monitoring the operating health of the unit, digitized at a sampling frequency of 2000 Hz. One day, the vibration at the second measuring point was abnormal shown in the monitoring system. A signal was taken from the system to analyze the exception reason, shown in Fig.7. The rotating frequencies of the high and low speed shafts are respectively 96.67 Hz and 23.63 Hz, which are dominant in the spectrum. We see from Fig.7(a) that the waveform in the time domain characterized as the fluctuant and asymmetrical sinusoidal signal mainly constrained by the rotating frequency of the high frequency. Moreover, the second harmonic frequency of the high shaft is also evident in the spectrum, indicating the unbalanced or/and misalignment faults in the unit. Owing to the dynamic balance processing before operation, the misalignment is diagnosed from the signal.

Using the proposed method, we analyze the signal to further detect the exception reason. Only $c_1(t)$ is chosen for the noise estimation, eliminating the redundant false component $c_5(t)$ from the original ENEMD. Due to the single IMF, the noise estimation by the local reconfiguration is performed. Fig.8 displays the refined results of IMF1 and IMF2 by the method. We see from Fig.8(a) that evenly spaced impulses exist in IMF1, highlighted by the downward-pointing arrows, the average interval time of which is about 0.031s. The feature frequency of the impulses is just consistent with the 1/3 fractional harmonic component of the high-speed rotating frequency. It is revealed that such fractional harmonic components are the symptoms of rub-impact faults for rotating machinery, especially in the early potential fault stage [18]. Meanwhile, the signal in Fig.8(b) is a typical sinusoidal signal, representing the vibration of the high speed shaft. Considering the prominent fractional harmonic fault features, it is conjectured that the rubbing-impacts existed in the unit close to the second measuring point.

After analyzing the structure of the unit, we found that the flue gas turbine and the fan were joined by a diaphragm coupling. To compensating the misalignment fault of the

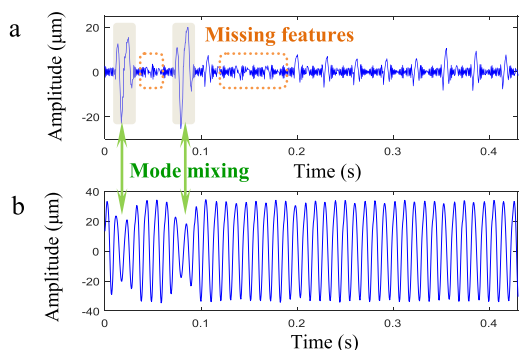


FIGURE 9. The refined results in case 2 by the original ENEMD: (a) IMF1; (b) IMF2.

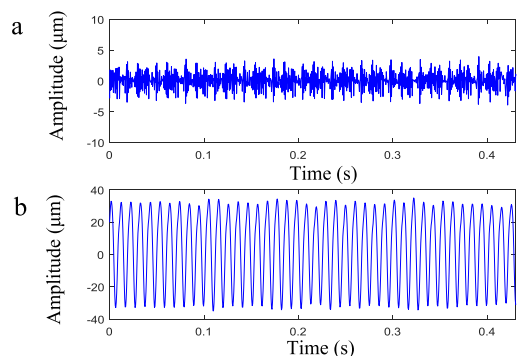


FIGURE 10. The refined results in case 2 by EEMD: (a) IMF1; (b) IMF2.

unit, the relative rubbing happened between the diaphragms. Furthermore, the misalignment fault also induced the local rubbing-impact faults between the shaft and the bearing bush.

The same signal is also processed using the original ENEMD, EEMD and EMD, shown in Figs.9-11. In the refined results by the original ENEMD in Fig.9, some weak impulses denoted in the dotted rectangles are unfortunately lost. Meanwhile, there exists mode mixing problem in the results. From Fig.10 by EEMD, we could not find any fault features supporting the diagnostic conclusion, although the mode mixing is well eliminated. The refined results by EMD in Fig.11 are similar to those in Fig.9, which are also lack of the sufficient evidence for the fault diagnosis. Apparently, the proposed method outperforms the contrastive methods, regardless of extracting the weak features or alleviating the mode mixing phenomenon.

V. CONCLUSION

ENEMD is an intelligent method by the nice integration of adaptively decomposing and naturally denoising. To improve the capability of extracting the weak fault features in rotating machinery, the dual-mode noise-reconstructed EMD is enhanced from the integrated ENEMD. The possible noise-only IMF selection rule is first redesigned according to the noise characteristic and the correlation evaluation, to address the issue of noise estimation deviation caused by the redundant false components. The adaptive local minimax threshold is then proposed in the noise estimation technique for a low

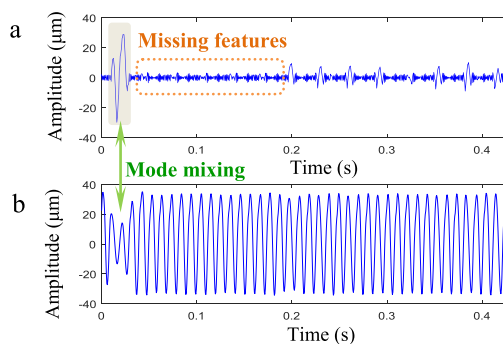


FIGURE 11. The refined results in case 2 by EMD: (a) IMF1; (b) IMF2.

SNR signal, to overcome the drawback of additionally keeping some critical but weak fault features into the estimation noise. Hereinto, every local threshold is respectively performed in each sliding window defined by the demodulated rotating-related feature frequency. Finally, the algorithm of dual-mode noise-reconstructed EMD is proposed with the flowchart.

Engineering case studies on the fault diagnosis for a hot strip finishing mill and a heavy oil catalytic cracking unit are used to demonstrate the effectiveness of the proposed method. The analytic results show that the method could effectively extract the periodic impulses and detect the potential local damage on the large gear at the early fault stage, despite the condition indexes within the normal limits from the monitoring system. Meanwhile, the method could successfully reveal the weak rubbing-impact faults along with alleviating the mode mixing phenomenon in the refined results for fault diagnosis of the heavy oil catalytic cracking unit. Hence, the method could provide a promising tool for weak feature extraction and fault diagnosis of rotating machinery.

ACKNOWLEDGMENT

The co-first author J. Yuan would like to gratefully thank her advisor Prof. Zhengjia He for his instruction and edification, which she benefits from in the whole life. (Jing Yuan and Huiming Jiang are co-first authors.)

REFERENCES

- [1] D. Wang, K.-L. Tsui, and Q. Miao, "Prognostics and health management: A review of vibration based bearing and gear health indicators," *IEEE Access*, vol. 6, pp. 665–676, 2018.
- [2] J. Ye, C. Chu, H. Cai, X. Hou, B. Shi, S. Tian, X. Chen, and J. Ye, "A multi-scale model for studying failure mechanisms of composite wind turbine blades," *Compos. Struct.*, vol. 212, pp. 220–229, Mar. 2019.
- [3] Y. Lei, J. Lin, Z. He, and M. J. Zuo, "A review on empirical mode decomposition in fault diagnosis of rotating machinery," *Mech. Syst. Signal Process.*, vol. 35, nos. 1–2, pp. 108–126, Feb. 2013.
- [4] S. Wang, I. W. Selesnick, G. Cai, B. Ding, and X. Chen, "Synthesis versus analysis priors via generalized minimax-concave penalty for sparsity-assisted machinery fault diagnosis," *Mech. Syst. Signal Process.*, vol. 127, pp. 202–233, Jul. 2019.
- [5] L. Wang, Z. Liu, Q. Miao, and X. Zhang, "Complete ensemble local mean decomposition with adaptive noise and its application to fault diagnosis for rolling bearings," *Mech. Syst. Signal Process.*, vol. 106, pp. 24–39, Jun. 2018.

- [6] Y. Wang, Z. Wei, and J. Yang, "Feature trend extraction and adaptive density peaks search for intelligent fault diagnosis of machines," *IEEE Trans. Ind. Informat.*, vol. 15, no. 1, pp. 105–115, Jan. 2019.
- [7] Z. Huo, Y. Zhang, P. Francq, L. Shu, and J. Huang, "Incipient fault diagnosis of roller bearing using optimized wavelet transform based multi-speed vibration signatures," *IEEE Access*, vol. 5, pp. 19442–19456, 2017.
- [8] N. E. Huang, Z. Shen, S. R. Long, M. C. Wu, H. H. Shih, Q. Zheng, N.-C. Yen, C. C. Tung, and H. H. Liu, "The empirical mode decomposition and the Hilbert spectrum for nonlinear and non-stationary time series analysis," *Proc. Roy. Soc. London A, Math., Phys. Eng. Sci.*, vol. 454, no. 1971, pp. 903–995, Mar. 1998.
- [9] Z. Wu and N. E. Huang, "Ensemble empirical mode decomposition: A noise-assisted data analysis method," *Adv. Adapt. Data Anal.*, vol. 1, no. 1, pp. 1–41, 2008.
- [10] F. Xu, X. Song, K.-L. Tsui, F. Yang, and Z. Huang, "Bearing performance degradation assessment based on ensemble empirical mode decomposition and affinity propagation clustering," *IEEE Access*, vol. 7, pp. 54623–54637, 2019.
- [11] L. Wang, G. Cai, J. Wang, X. Jiang, and Z. Zhu, "Dual-enhanced sparse decomposition for wind turbine gearbox fault diagnosis," *IEEE Trans. Instrum. Meas.*, vol. 68, no. 2, pp. 450–461, Feb. 2019.
- [12] C. Wang, H. Li, G. Huang, and J. Ou, "Early fault diagnosis for planetary gearbox based on adaptive parameter optimized VMD and singular kurtosis difference spectrum," *IEEE Access*, vol. 7, pp. 31501–31516, 2019.
- [13] J. Yuan, Z. He, J. Ni, A. J. Brzezinski, and Y. Zi, "Ensemble noise-reconstructed empirical mode decomposition for mechanical fault detection," *J. Vib. Acoust.*, vol. 135, no. 2, 2013, Art. no. 02101.
- [14] J. Yuan, F. Ji, Y. Gao, J. Zhu, C. Wei, and Y. Zhou, "Integrated ensemble noise-reconstructed empirical mode decomposition for mechanical fault detection," *Mech. Syst. Signal Process.*, vol. 104, pp. 323–346, May 2018.
- [15] P. Flandrin, P. Goncalves, and G. Rilling, "EMD equivalent filter banks, from interpretation to applications," in *Hilbert-Huang Transform and Its Applications*, N. E. Huang and S. S. P. Shen, Eds. Singapore: World Scientific, 2005, pp. 67–87.
- [16] D. L. Donoho and I. M. Johnstone, "Minimax estimation via wavelet shrinkage," *Ann. Statist.*, vol. 26, no. 3, pp. 879–921, 1998.
- [17] S. Mallat, *A Wavelet Tour of Signal Processing*, 2nd ed. New York, NY, USA: Academic, 1999.
- [18] Z. K. Peng, F. L. Chu, and P. W. Tse, "Detection of the rubbing-caused impacts for rotor-stator fault diagnosis using reassigned scalogram," *Mech. Syst. Signal Process.*, vol. 19, no. 2, pp. 391–409, 2005.



JING YUAN received the Ph.D. degree in mechanical engineering from Xi'an Jiaotong University, in 2011. From 2011 to 2018, she was a Senior Engineer with the Shanghai Academy of Spaceflight Technology. Since 2018, she has been an Associate Professor with the School of Mechanical Engineering, University of Shanghai for Science and Technology. Her current research interests include mechanical condition monitoring, fault diagnosis, signal processing, and feature extraction.



HUIMING JIANG received the B.S. degree in mechanical engineering from Xi'an Jiaotong University, in 2011, and the Ph.D. degree in mechanical engineering from Shanghai Jiao Tong University, in 2017. She is currently a Lecturer with the School of Mechanical Engineering, University of Shanghai for Science and Technology. Her current research interests include machinery condition monitoring and fault diagnosis, intelligent fault diagnostics, and performance degradation assessment.



QIAN ZHAO received the Ph.D. degree in mechanical engineering from Northeastern University, in 2016. She is currently a Lecturer with the School of Mechanical Engineering, University of Shanghai for Science and Technology. Her current research interests include rotating machinery dynamics and vibration control.



CHONG XU received the B.E. degree from the School of Mechanical Engineering, Hubei University of Arts and Science, Xiangyang, China, in 2018. He is currently pursuing the M.E. degree with the School of Mechanical Engineering, University of Shanghai for Science and Technology. His current research interests include mechanical signal processing and feature extraction.



HAIJIANG LIU received the Ph.D. degree in mechanical engineering from Chongqing University, in 1995. He is currently a Professor with the School of Mechanical and Power Engineering, Tongji University. His current research interests include precision measurement and control, and digital manufacturing technology and application.



YONGXIANG TIAN received the Ph.D. degree in vehicle engineering from Tongji University. He has been working with the Shanghai Fire Research Institute of MEM and the China National Fire-Fighting Equipment Quality Supervision Testing Center, since 2007. He is mainly engaged in the technical research and development and testing of fire fighting vehicles and other equipment.

...